2025

# Development of mouse models of multisystemic histiocytosis-like disease with bone involvement

BOSTON UNIVERSITY

ARAM V. CHOBANIAN & EDWARD AVEDISIAN SCHOOL OF MEDICINE

Thesis

# DEVELOPMENT OF MOUSE MODELS OF MULTISYSTEMIC HISTIOCYTOSIS-LIKE DISEASE WITH BONE INVOLVEMENT

by

**DARAH ROSE-MERLIE DEROLY**

B.S., University of Connecticut, 2022

Submitted in partial fulfillment of the

requirements for the degree of

Master of Science

2025

Approved by

First Reader

Beth Bragdon Ph.D.
Assistant Professor of Orthopaedic Surgery

Second Reader

Christian E. Jacome-Galarza, Ph.D.
Instructor, Harvard Medical School
Brigham and Women's Hospital

## DEDICATION

*To Mom and Dad, for supporting me every step of the way.*

## ACKNOWLEDGMENTS

First, I would like to thank my P.I., Christian Jacome-Galarza for giving me the opportunity to complete my thesis in his lab. I am also grateful to Jenna Taylor for taking the time to teach me throughout this project. Additionally, I want to thank my fellow MAMS classmate, Jorge Rodriguez, for always being willing to help whenever he could. I would also like to express my appreciation to the Gravellese lab for their support.

A special thank you to Camelia Hacein-Bey for laying the groundwork that made my project possible. I am also sincerely grateful to Dr. Sundeep Khosla and Dr. David Monroe for generously providing the lab with the *CathepsinK*$^{CreERT2}$ mouse model.

Finally, I want to thank my program director, Dr. Gwynneth Offner, for her invaluable knowledge, insight, and advice throughout my two years in the Master's in Medical Science program.

**DEVELOPMENT OF MOUSE MODELS OF MULTISYSTEMIC HISTIOCYTOSIS-LIKE DISEASE WITH BONE INVOLVEMENT**

**DARAH ROSE-MERLIE DEROLY**

ABSTRACT

Histiocytosis features the aberrant functions of macrophages, osteoclasts, and other cells of hematopoietic origin. It has an extensive range of phenotypic presentations involving single organ or multiple organs. The bone phenotype of histiocytosis, the most prominent in juvenile cases, is in most cases aggressive and lethal. Current treatments available are broad and have limited effectiveness. The BRAF gene is an oncogene involved in the mitogen activated protein kinase (MAPK) pathway. A point mutation in the *BRAF* gene resulting in replacement of valine (V) to glutamine (E) at the aminoacidic position 600 results in constitutive activity generally common in cancers and Langerhans cell histiocytosis. Exploration of more specific treatment methods for histiocytosis targets the BRAF V600E mutation. Here we work on developing and testing new mouse models that express BrafV600E mutations. Further analysis of the fluorescent labeling efficiency of tamoxifen inducible mouse model will be completed before proceeding to inducing histiocytosis-like disease with bone involvement in mice.

## TABLE OF CONTENTS

## LIST OF TABLES

## LIST OF FIGURES

## LIST OF ABBREVIATIONS

ACK ..... Ammonium-Chloride Potassium

BSA ..... Bovine Serum Albumin

CTSK ..... Cathepsin K

EMPs ..... Erythro-myeloid progenitors

FACS ..... Fluorescence Activated Cell Sorting

HSCs ..... Hematopoiesis Stem Cells

IACUC ..... Institutional Animal Care and Use Committee

MAPK ..... Mitogen Activated Protein Kinase

OCT ..... Optimal Cutting Temperature

OcMDC ..... Osteoclasts/Macrophages/Dendritic Cell Progenitor

OCs ..... Osteoclasts

PCR ..... Polymerase Chain Reaction

TRAP ..... Tartare-Resistant Acid Phosphate

YFP ..... Yellow Fluorescent Protein

4-hydroxytamoxifen ..... 4-OH Tamoxifen

# INTRODUCTION

Histiocytosis is a multisystemic condition characterized by proliferation and accumulation of inflammatory cells. The mechanism of action features the aberrant functions of macrophages, osteoclasts (OCs), and other cells of hematopoietic origin[1]. As named by its defining characteristic, the term histiocyte of histiocytosis refers to "cells of the tissue" which is used to refer to phagocytic cells that are involved in triggering pathological features associated with histiocytosis[1]. Histiocytosis pathology can be presented in an extensive range of manifestations, varying from mild to severe life-threatening cases. Typical presentations can involve a single organ or be multisystemic in phenotype [2,1]. Common organs or systems involved can include the brain, skin, lungs, liver, spleen, and skeleton [2]. Affected organs suffer from inflammatory lesions, granuloma formation, or even exacerbated bone resorption caused by osteoclasts in localized or systemic anatomical areas. The combination of affected organs can vary from case to case and some forms of the disease are more aggressive than others.

The bone phenotype of histiocytosis in particular is especially aggressive and lethal[3]. The clinical extent of this phenotype carries variance amongst adults and typically less severe than cases diagnosed in young children[2,4,5]. Approximately 75-80% of children with histiocytosis carry some sort of bone phenotype which makes it one of the most prominent phenotypes found in juvenile cases[3]. The annual incidence of histiocytosis in children under the age of 14 is 4.6 per million[3]. While lesions due to histiocytosis can be found in all bones, around 50% of all bone lesions occur in flat bones [3]. With the lesions on long bones, the femurs, tibia and humeri are the most likely probable sites[3]. The

formation of these lesions on the bones, which are caused by the stimulation of osteoclasts by cytokines and chemokines, can be extremely painful and the available treatments are limited [2,6,7]. Lastly, the location of these lesions can lead to additional problems, including tooth loss due to lesions in the mandible and structural changes and inflammation due to intracranial lesions [6].

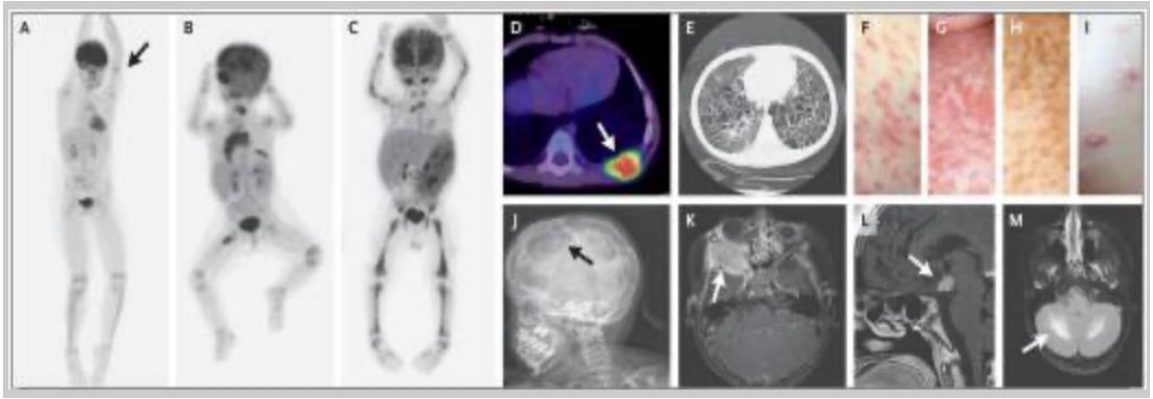


**Figure 1. Clinical phenotypes of Histiocytosis**
Panels A-C and J-M show possible bone phenotypes formed by osteoclasts in patients of histiocytosis. A-C shows progressively worsening presentation, varying from a single lesion to multiple lesions in different bones. Panels D-I show the different presentations seen in soft tissue formed by either macrophages or Langerhans cells (Allen et al, 2018).

It is also exceedingly difficult to diagnose due to shared similarities to other diseases, and difficulty with identifying bone lesions [2]. Common methods of diagnosis include radiographic imaging or a bone biopsy [3]. However, there are significant limitations to these methods. Bone biopsies can be one of the more effective methods but carries added risk of unsavory side effects or complications[1]. Due to this, imaging remains the predominately used system for diagnosis. This is mostly ineffective as the bone lesions can be difficult to fully characterize without lab analysis [3]. These factors, along with the

potential of fundamental or permanent deformities make the prognosis of bone involved histiocytosis extremely poor.

The current treatments available for the disease, especially in relation to bone lesions, also present a challenge. Most of these treatments are broad, carry added risks, and have limited effectiveness[8]. Bisphosphonates and other osteoclasts inhibitors tend to be the standard for treatment of bone lesions, along with limited causes in which chemotherapy regimens are used [8,9]. Patients are typically treated with bisphosphonates for a period of time until reaching the maximum effect in 3-6 months of continued treatment [10]. Bisphosphonates have been found to decrease the severity of bone lesions and provide relief for the pain that is associated with them [8]. While mostly effective, the treatment time varies from patient to patient[8]. Additionally some patients do not respond to them or have more rapid rebounding effect after cessation [8]. The broad approach applied with treating histiocytosis makes it difficult to avoid or control potentially harmful side effects. For more specified treatment, other options need to be considered.

The exploration of these more specific treatment methods essentially takes into account the origin of osteoclasts and other inflammatory cells. During embryonic development, hematopoiesis occurs in the yolk sac [11]. The erythro-myeloid progenitors (EMPs) formed during this period can give rise to different tissues resident macrophages, and osteoclasts [12]. Tissue resident macrophage populations are established during embryogenesis, they replenish themselves independently of bone marrow hematopoiesis [12]. Later during development, the site of hematopoiesis

is primarily the bone marrow. This can give rise to a new subset of macrophages derived from hematopoietic stem cells (HSCs) [12].

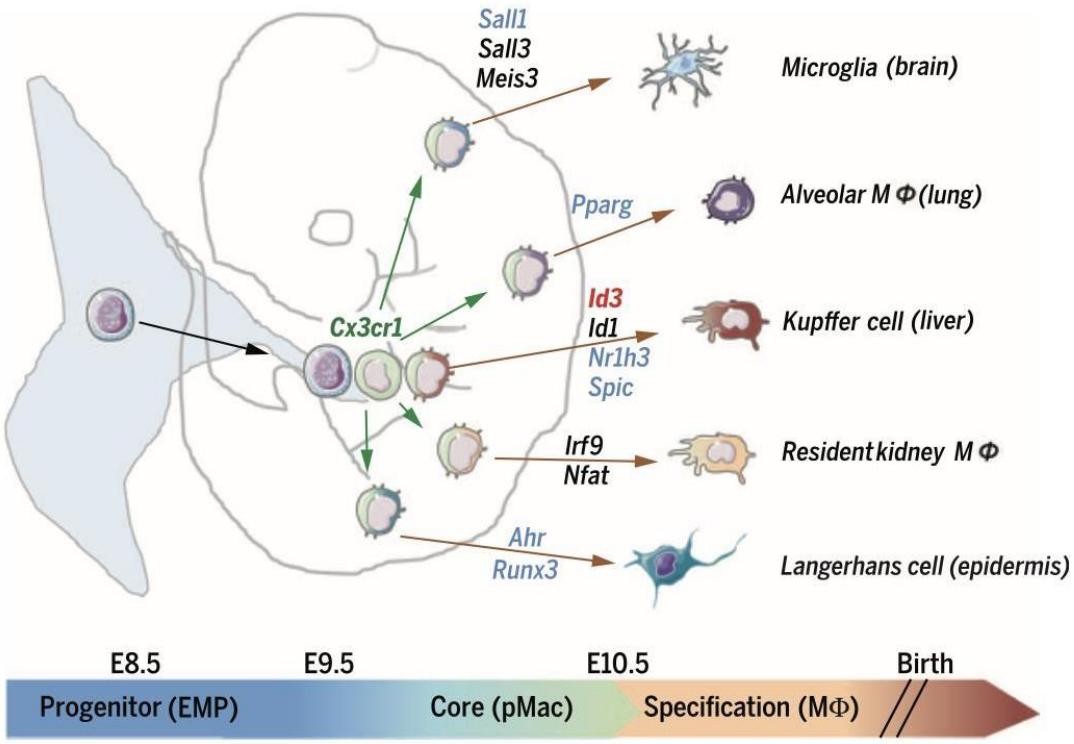


**Figure 2. Initial model of the origins of systemic macrophages and tissue resident macrophages.**
Models shows the erythromyeloid progenitor (EMP) differentiation through Cx3cr1 giving rise to different tissue resident macrophages (Mass et al, 2016)

Initially, it was thought that osteoclasts originated solely from bone marrow HSCs, specifically monocytes [13]. This was mostly due to their location and perceived similarity to the bone building cells or osteoblasts [13]. Assuming that this was true, it would have been a significant challenge to develop targeted treatment for multisystem histiocytosis. However, it was later discovered that macrophages and osteoclasts share the same

progenitor which was reported as the osteoclasts/macrophage/dendritic cell progenitor or OcMDC [14]. Unlike tissue resident macrophages, where they can only be replenished by cell division of the initial seeding of EMPs during embryogenesis, osteoclasts can be produced by both EMPs and HSCs [14].

## Braf functions and mutations in the Braf gene

The *BRAF* gene is an oncogene involved in the mitogen activated protein kinase (MAPK) pathway [15]. This pathway is essential in regulating many cell functions such as growth, cellular proliferation and apoptosis [16]. Proper regulation of the MAPK pathway prevents uncontrollable cell division that could eventually be damaging. However, a point mutation in the *BRAF* gene resulting in replacement of valine (V) to glutamine (E) at the aminoacidic position 600, can result in the *BRAF* gene remaining constitutively active and in turn maintaining the downstream signaling pathway[15 17]. This mutation, BRAF V600E, affects the regulation of signaling of proteins such as RAS proteins and GTPases [16]. Due to this, the BRAF V600E mutation is a hallmark of many cancers [15 16].

While the BRAF V600E mutation is generally common in cancers with RAS mutations, it is more prevalent in malignant melanomas [15]. Approximately 40-50% of malignant melanoma patients carry the BRAF V600E mutation. This presents an additional challenge when diagnosing Langerhans cell histiocytosis. According to the literature, histiocytosis is considered a neoplastic disorder of myeloid originated cells [18]. Although similar, lesions formed by other malignant histiocytic diseases such as

histiocytic sarcoma or malignant histiocytosis, are typically more aggressive than those found in Langerhans cells histiocytosis [1].

The level of malignancy and fatality displayed by the disease can also be attributed to whether the BRAF V600E mutation is present within the affected cells [1]. This along with the BRAF V600E mutation being found in approximately 38% to 64% of all Langerhans cells histiocytosis cases, has sparked the debate of whether to consider it a cancer [1,17]. Additionally, many symptoms of histiocytosis can be treated by both methods that treat cancer - such as chemotherapy- and methods used to treat autoimmune conditions, such as prednisone and vinblastine[1].

Targeting the BRAF V600E mutation for treatment of melanomas has been the goal of many research projects since it was first identified [18]. With most medications carrying several side effects, medicine has been making a conscious effort of personalizing treatments to provide the most efficient care to patients. However, this move towards precision medicine has not translated towards research of histiocytosis. Perhaps, the development of new animal models that recapitulate multisystemic disease might be beneficial for drug testing. Although, there are many reports of murine models that express BrafV600E mutations under the control of tissue specific lines, there are no reports with bone involvement and aberrant osteoclast activity resulting in exacerbated pathological bone resorption. In this work, we explore the potential of some animal models to generate histiocytosis-like-disease with bone involvement.

## Mouse Models

Usually, research projects involving severe diseases like histiocytosis use models for more in depth pre-clinical studies. Mouse models in particular are often used because approximately 95% of genes found in mice are homologous to human genes [19] This allows for testing of treatment methods *in-vivo* before attempting to apply them clinically. Furthermore, a mouse model for a given disease can contribute to building more scientific knowledge and understanding of pathological mechanisms of disease [19].

Although there are various benefits for their usage, it has been difficult to create a mouse model with the full presentation of the disease. Histiocytosis is a single system or multisystemic disease with affects in several organs, so it is necessary to have a model displaying all the potential phenotypes for effective studies. We know that macrophages and osteoclast may share the same progenitor, but targeting all of these cells to create a mouse model for multisystem histiocytosis is still a working progress.

Some mouse models for histiocytosis that have been developed thus far have had limited success in targeting all the systems and organs affected by histiocytosis. Certain models, such as $Langerin^{Cre}; BRAF^{LSL}\text{-}V600E$ have had some success with inducing the BRAF V600E mutation in Langerhans cells affecting skin, and also other organs like lungs and liver [20]. Another model, $CD11c^{Cre}; BRAF^{LSL\text{-}V600E}$ also showed promising results with the labeling of dendritic cells in the lungs and liver [20]. Additionally, the $Csf1r^{MeriCreMer};BRAF^{LSL\text{-}V600E};Rosa26^{LSL\text{-}YFP}$ induced the BRAF V600E mutation within microglia resulting in a neurodegenerative phenotype emerging approximately by 4 months after 4OH-tamoxifen injection [12]. The closest model for multisystem histiocytosis

is the *BRAF*-V600E*Scl*$^{+}$ model created by pulsing with tamoxifen at 8 weeks old [21]. This showed histiocytosis-like disease with mutation induced labeling of lungs, skin, spleen, and liver. Its results were also indicative of the labeling of hematopoietic stem cells [21]. There is a mention of a potential bone phenotype in this model, but the results presented do not fully characterize this.

We have made a few attempts to characterize this phenotype. The goal is not only to create a constitutive model but also one that can be induced if desired. The Cre/loxP system plays a significant role in achieving this. The mechanics of this system are centered around Cre being a recombinase that recognizes loxP sites [22]. The genes of interests are typically flanked between two loxP sites [22]. This allows for the removal or inversion of particular sequences within the DNA [22]. This arrangement is facilitated by targeting the gene sequence of interest to knock it in within the loxP sites [22]. Crossing of these mice with a mouse expressing Cre recombinase, will eventually produce a mouse that has the targeted gene knocked out [22]. While this system alone can be extremely beneficial in studying disease in mice, it is more ideal to have a system that is inducible. To generate murine models carrying the BRAF V600E mutation in cells such macrophages and/or osteoclasts for their use in drug testing, we first tested their potential to carry the mutation by analyzing tissue specific mouse lines.

The Cre/loxP system can be constitutive (always active) or inducible which can activate Cre recombination by induction through a modified an estrogen receptor (ER) and tamoxifen (an estrogen antagonist)[23]. Activation of this process occurs once tamoxifen has been administered to a mouse carrying the inducible Cre construct [22]. This

allows the Cre protein translated to translocate in the nucleus for interaction with the loxP sites[23]. Processes such as fluorescent protein reporter for cell lineage tracing, the deletion of a given gene of interest, or the activation of desired mutation at any given timepoint can now occur. In our particular case, our aim is to induce a Braf mutation in osteoclasts utilizing tamoxifen to induce the Cre recombination in osteoclast-specific mouse models (i.e., Cathepsin K promoter). We will utilize both, a Cre reporter in which Cre activates the transcription of the fluorescent protein YFP to determine expression of the promoter, this permanently labels the cells of interest with a fluorescent marker that can be detected through immunofluorescent staining and fluorescent microscopy. Ultimately, we will use these models to induce Braf mutations in Cathepsin K (or other markers) expressing cells.

There has been some previous success with the labeling osteoclast progenitors using this system. Specific markers on the surface of osteoclasts can be identified and fused with a Cre recombinase [22]. For the goal of creating a mouse model of multisystem histiocytosis with bone involvement, we have explored the *Cx3cr1*$^{CreERT2}$ mouse model, which has shown promising results [24]. The first step in creating this model involved permanently labeling the desired cell types with the fluorescent YFP reporter, *Rosa26*$^{LSL\text{-}YFP}$. This provides a tool to identify cells, their anatomical locations and to determine cell function [25]. This reporter mouse was used to test the efficiency and specificity to label cell that arise from erythro-myeloid progenitors (EMP), including tissue resident macrophages and osteoclasts [11,24].

**Table 1. Labeling efficiency of the Cx3cr1$^{CreERT2}$; R26$^{LSL-YFP}$ model.** The percentage of labeled EMP derived cells in various organs. (Adapted from Hacein- Bey)

| Cell Type | Percentage Labeled |
|---|---|
| Kupffer Cells | 6.5% |
| Kidney Macrophages | 3.0% |
| Lung Macrophages | 2.0% |
| Microglia | 85% |

The *Cx3cr1$^{CreERT2}$; R26$^{LSL-YFP}$* model showed notable labeling of Kupffer cells (liver tissue resident macrophages), kidney macrophages, lung alveolar macrophages and microglia (**See table 1**) [24]. Additionally, no labeling of hematopoietic stem cells (HSC) or other non-target cells was found [24]. The efficiency and moldability of this labeling system make this model an ideal candidate for our studies.

Since this reporter system was proven to be somewhat efficient in labeling macrophages and very efficient in labeling embryonic osteoclasts, the next step is to increase its efficiency by increasing tamoxifen dosage. Then we will use it for activation of the BRAF V600E mutation macrophages and osteoclast. We know from previous work, utilizing *Csf1r$^{Mer\text{-}iCre\text{-}Mer}$* mouse model, that as little as 20-30% of microglia will express the Braf-V600E mutations resulting in partial paralysis of the hindlimbs in 4–6-month-old mice [12]. Therefore, we expect this model to have a similar effect, with potential bone phenotype during mouse development.

Generation of mouse model with multisystem histiocytosis has been done before with varying levels of success. However, there is no current known model expressing multisystem histiocytosis with bone involvement. The bone phenotype of histiocytosis is one of the most lethal phenotypes of the disease [1]. The lack of a proper model has made it difficult to effectively study the disease. The development of an effective and workable model with a bone phenotype will provide an avenue for studying the disease mechanism of action and for the testing of new potential treatment methods.

The goal of thesis is centered around filling this gap identified from the previous mouse models created to study the disease models. We will present Cre inducible models with potential to generate various levels of histiocytosis pathology., some with an embryonic induction of EMP-derived progenitors and others with a more narrow specificity for all osteoclasts, regardless of their origin (embryonic or adult bone marrow), and some macrophages (lung and skin).

## SPECIFIC AIMS

1. **Generation of a new mouse model of histiocytosis-like disease with bone involvement.**

To generate this model first, we will test the efficiency and specificity of a recently developed mouse model to target osteoclasts. Based on previous reports and testing, induction of Cre recombination is lethal 12 days after birth. Preliminary data for a milder form was generated and tested for YFP expression under control of CathepsinK$^{\text{CreERT2}}$ in the tissues of interest. Therefore, we will analyze and determine the fluorescent labeling efficiency and specificity of two mouse models: 1) tamoxifen inducible in mouse pups (at P7-8) and 2) compare to constitutively expressed *CathepsinK$^{Cre;}$Rosa26$^{LSL\text{-}YFP}$* during development (pups to adult mice). The goal of this aim is to establish the requirements for the tamoxifen-inducible model before proceeding to inducing histiocytosis-like disease with bone involvement in mouse pups (i.e., *CathepsinK$^{CreERT2;)}$*. This will allow for generation of a milder form of disease compared to our previously reported model (*CathepsinK$^{Cre;}$Braf$^{LSL\text{-}V600E}$* pups who perish around postnatal day 12) [26], and monitoring of disease progression and testing of new therapeutic targets.

**2. Generate a new mouse model of multisystem histiocytosis with bone involvement.**

Based on the available literature, multisystemic histiocytosis with bone involvement has not been fully characterized in any of the currently available mouse models. The closest to such a model showed potential osteolytic lesions however bone involvement was not reported. We aim to generate a mouse model that will display the phenotype of multisystem histiocytosis with the desired bone phenotype, at least during early stages of postnatal development. To do this, we examine a previously reported model form our lab that labels tissue resident macrophages and embryonic osteoclasts, in cell lineage tracing studies, as discussed above. This model utilizes the *Cx3cr1*$^{CreERT2}$ tamoxifen inducible mouse model[24]. Therefore, we will use this *Cx3cr1*$^{CreERT2}$ mouse model and cross it with *Braf*$^{LSL\text{-}V600E}$ mice to generate *Cx3cr1*$^{CreERT2}$*;Braf*$^{LSL\text{-}V600E}$ mice that will result in the expression of *Braf- V600E* mutations in tissue resident macrophages and embryonic osteoclast. This model has not been previously generated and promise to provide with a potential mouse model of histiocytosis-like disease with bone involvement. Here, we will focus on evaluating the efficiency of such model to induce changes in osteoclast phenotype and resorptive capacity during early bone development.

# METHODS

## Animal Facilities

The mice used for these experiments were kept and bred at the Brigham and Women's Hospital Center for Comparative Medicine animal facility. The facility follows a strict guideline of a 12 hour 7 am to 7 pm daylight access schedule to maintain a healthy circadian rhythm for the animals. They are fed a controlled diet after weaning from their mothers and monitored carefully for signs of malnutrition or sickness. Mice identity is determined through ear tags for older mice and ear notches or tail clips for younger mice. All experiments performed on these mice were in agreement with the approved IACUC protocols and guidelines for ethical treatment of animals. Euthanizing methods used during all experiments were humane and painless with secondary methods for confirmation because any proceeding steps in the experiments.

## Genotyping

Genotyping of the mice is performed prior to every experiment and confirmed after experiments, as needed. Samples for genotyping are collected by clipping approximately 2mm of tissue from the tail of each mouse in a labeled Eppendorf tube. DNA is extracted by adding 300 μL of 50mM Sodium Hydroxide to each tube and heating the sample at 98C for 30 minutes. Samples are then mixed and returned to heat for another 30 minutes to insure sufficient lysis of the tissue. Following this, the sample is neutralized by the addition of 30 μL 1M Tris-HCL. Each tube is centrifuged to form a pellet at the bottom.

The supernatant of each sample is then collected and transferred to a new tube (DNase free) in preparation for the PCR (polymerase chain reaction).

Genotyping is performed for the genes of interest with their respective primers as shown in (**See Table 2**). Each gene being identified requires its own primer along with a positive control and a wildtype DNA sample. Once the primers have been selected, a mastermix is created for each gene. A master mix contained, DreamTaq, nuclease-free water, the primer combinations and the DNA being amplified. The standard PCR reaction requires approximately 20 μL of volume spread in a specific ratio of each component of the mastermix. These volumes are then multiplied by the number of samples being analyzed with consideration for 2-3 extra samples to account for pipetting error.

**Table 2. Primers for genes of interest.**

| Gene | Nucleotide sequence 5'→ 3' |
|---|---|
| *CatK*$^{CreERT2}$ → Forward | CAA GTT TCT GCT GCT ACC CA |
| *CatK*$^{CreERT2}$ ← Reverse | TAG AGC CTG TTT TGC ACG TT |

| Gene | Nucleotide sequence 5'→ 3' |
|---|---|
| *CathepsinKCre 1* | TTATTCCTTCCGCCAGGATG |
| *CathepsinKCre 2* | TTGCTGTTATACTGCTTCTG |
| *CathepsinKCre 3* | TAGTTTTTACTGCCAGACCG |

| Gene | Nucleotide sequence 5'→ 3' |
|---|---|
| *Rosa26LSL-YFP 1* → Forward | AAG TCG CTC TGA GTT GTT AT |
| *Rosa26LSL-YFP* 2 WT← Reverse | GGA GCG GGA GAA ATG GAT ATG |
| *Rosa26LSL-YFP* ← Reverse | GCG AAG AGT TTG TCC TCA ACC |

| Gene | Nucleotide sequence 5'→ 3' |
|---|---|
| *BrafLSL-V600E* 1 → Forward | TGA GTA TTT TTG TGG CAA CTG C |
| *BrafLSL-V600E* 2 ← Reverse | CTC TGC TGG GAA AGC GGC |

| Gene | Nucleotide sequence 5'→ 3' |
|---|---|
| *Cx3cr1*$^{CreERT2}$ → Mutant Forward | GTT AAT GAC CTG CAG CCA AG |
| *Cx3cr1*$^{CreERT2}$→ WT Forward | AGC TCA CGA CTG CCT TCT TC |
| *Cx3cr1*$^{CreERT2}$ ← Reverse | ACG CCC AGA CTA ATG GTG AC |

**Table 3. Mastermix preparations and volumes.** Numbers account for one standard PCR reaction with a total of 20 μL of volume. (Adapted from Hannah Nelson)

| **Standard PCR reaction** | **Volume Added (20μL total)** |
|---|---|
| DreamTaq | **10μL** |
| Nuclease-free water | **7.4μL** |
| Primer combination | **1.6μL** |
| DNA | **1μL** |

After PCR amplification, samples are taken for analysis via gel electrophoresis. A 1.5% agarose gel is prepared with SYBR safe DNA gel stain. Gel size, run time, along with volumes used for the components of the gel varies by the number of samples being analyzed (**See Table 4**). However, the preparation methods used remain the same. The appropriate volume of 1X TBE buffer is added to an Erlenmeyer flask with the corresponding amount of agarose powder (**See Table 4**). The mixture is heated for 2-3 minutes in a microwave until all the components are uniform. SYBR safe DNA gel stain is added, and the solution is poured into a gel tray. The gel is then covered in 1X TBE before the PCR products for each sample is added to the wells. Results are analyzed and compared to the wildtype and positive controls for each gene.

**Table 4. Gel electrophoresis size guide.** Total volume of 1x TBE, SYBR safe DNA stain and amount of agarose powder associated with each gel size. Run time also varies according to the size (Hannah Nelson)

| Gel tray size | Volume of 1x TBE | Agarose | SYBR safe DNA | Run time |
|---|---|---|---|---|
| 6-10 wells | 50 ml | 0.75 g | 2.25 ul | 30 min |
| 2 rows (10-14 wells) | 75 ml | 1.13 g | 3.5 ul | 30-45 min |
| 2 rows (10-20 wells) | 125 ml | 1.88 g | 6 ul | 45 min |
| 2 rows (16 wells) | 175 ml | 2.63 g | 8 ul | 45 min-1hr |
| 2 rows (20-30 wells) | 125 ml | 1.88 g | 6 ul | 30 min |

## Pulsed Labeling

*CathepsinK*$^{CreERT2}$;*Rosa26*$^{LSL\text{-}YFP}$ pups are genotyped to determine if they contain a copy of the Cre gene and YFP gene. At P7-P8, the pups are weighted prior to the 4-

hydoxytamoxifen (4OH tamoxifen) injections. Based on the weight of the mice, calculations are made to ensure that each mouse is receiving 200μg/g of 4OH tamoxifen supplemented with 100 μg/g of progesterone. To prepare 4-hydroxytamoxifen, 25 mg of powder is diluted in 250μL of 100% ethanol and vigorously vortex for approximately 2 minutes. Then 2250μL of sunflower oil are added to the solution and the mix is then sonicated for 30 minutes then vortex for 2 minutes and sonicated again for 30 minutes to yield a stock solution of 10mg/mL. Progesterone is prepared by diluting 25mg in 2.5mL of sunflower oil and gently vortex until dissolved (~1 min). Tamoxifen and progesterone are brought to room temperature before mixing to generate the final emulsion that will be used to inject mice. The mixture is drawn up in syringes assigned to each pup. Between 6-7 pm, each pup is carefully injected in the peritoneal cavity and monitored shortly for potential leaks. However, data observations do not rely on a specific time for injection. The pups are then observed daily for signs of potential illness before samples are collected from them.

## Sample Collection

The mice are euthanized at the Brigham and Women's Hospital through $CO_2$ asphyxiation for 15-20 minutes. They are kept in the chamber for an additional 5 minutes to confirm that expiration has occurred. A secondary method of cervical dislocation is performed before experimentation. Mice that were injected with 4OH tamoxifen are also weighted before euthanasia. Alternatively, certain experiments require the collection of peripheral blood and bone marrow. In this scenario, the mice are sedated with ketamine

and xylazine. Once they have been fully sedated, blood is collected through cardiac puncture and the secondary method of cervical dislocation is also be performed. Samples of choice are harvested using dissection techniques. Tissue samples collected typically include the brain, skin, liver, lungs, femurs, tibias and humeri and bone marrow from these bones and prepare for either histology or flow cytometry. For histology, the tissues collected are transferred to 4% formaldehyde in PBS for fixing. Soft tissues are kept in the 4% formaldehyde solution for 24hrs, and bone samples are kept in for 3 days at 4°C.

Following proper fixation of the tissues, soft tissues are moved to 30% sucrose while the bones samples are prepared for decalcification. Bones are decalcified in 14% EDTA for a total of 10 days for adult mice and 1 day for >P15 pups. The 10-day decalcifying process requires a change of 14% EDTA every 3 days allowing for a total of 3 changes. After the bone have been thoroughly decalcified, they are washed with water and moved to 30% sucrose in preparation for further analysis.

## Sample Preparation for Frozen Histology

Decalcified bone samples are frozen with dry ice in optimal cutting temperature (OCT) filled plastic molds. Once the samples have been sufficiently frozen, they are cut using a Cryostat Leica CM3050S at -20°C. Each sample is cut into 16μm sections onto cryostat tape. The tapes are then placed on slide and left to dry at 4°C for at least 48 hours. The sections will remain stored at 4°C until staining.

## Immunofluorescence Staining

For immunofluorescence staining, the fully dried sections are moved to room temperature and allowed to equilibrate for 30 minutes. Primary and secondary antibodies are chosen based on desired staining (**See Table 5, 6,7**). All antibodies are diluted in; 0.25% Bovine Serum Albumin or BSA, and 0.3% triton in PBS (PBT). The sections are rehydrated with PBS for 5 minutes with 3 changes of the PBS followed by a wash with PBT. The sections are then incubated at room temperature for 45 min with normal goat serum (Life Technologies, PCN 5000) diluted in PBT. The sections are washed 3 times with PBT and incubated with Streptavidin and Biotin at room temperature for 15 minutes each. Two washes of PBS are performed between the Streptavidin and Biotin incubations.

The primary antibodies selected are prepared and diluted in PBT. The sections are incubated for 15hrs at 4°C covered while covered with a small strip of parafilm to prevent dehydrating. The slide chamber is also covered in a thin layer of water to control moisture. The next day, the sections are left at room temperature for 30 minutes and washed with PBS before the secondary antibodies are added. Secondary antibodies typically incubate for 2 hrs. The sections are then fluorescently TRAP stained for 15 minutes under a UV light. Additionally, To-Pro-3 is used for nuclear staining in a 1:10,000 dilution in PBS. Nuclear staining incubates at room temperature for 10 minutes before the slides are mounted with 75% glycerol.

**Table 5. Antibodies used for immunofluorescence staining.** These antibodies are used for the immunofluorescence staining of frozen histology sections.

| Type | Host | Conjugation | Dilution | Source | Catalog # | Incubation |
|---|---|---|---|---|---|---|
| 1° | Goat | Biotin | 1::50 | Abcam | Abcam6658 | 15hrs at 4°C |
| 2° | Streptavidin | AlexaFluor488 | 1::100 | ThermoF | S-11223 | 2hrs RT |

**Table 6. Antibodies used for Ly6C monocyte immunofluorescence staining.** These antibodies are used for the immunofluorescence staining of frozen histology sections.

| Type | Host | Conjugation | Dilution | Source | Catalog # | Incubation |
|---|---|---|---|---|---|---|
| 1° | Goat | Biotin | 1::50 | Abcam | Abcam6658 | 15hrs at 4°C |
| 2° | Streptavidin | AlexaFluor488 | 1::100 | ThermoF | S-11223 | 2hrs RT |

| Type | Host | Fluorochrome | Dilution | Source | Catalog # | Incubation |
|---|---|---|---|---|---|---|
| 1° | Rat | Unconjugated | 1::100 | Abcam | Abcam6658 | 15hrs at 4°C |
| 2° | Goat | AlexaFluor405 | 1::50 | ThermoF | S-11223 | 2hrs RT |

**Table 7. Antibodies used for murine macrophage F4/80 immunofluorescence staining.** These antibodies are used for the immunofluorescence staining of frozen histology sections.

| Type | Host | Conjugation | Dilution | Source | Catalog # | Incubation |
|---|---|---|---|---|---|---|
| 1° | Goat | Biotin | 1::50 | Abcam | Abcam6658 | 15hrs at 4°C |
| 2° | Streptavidin | AlexaFluor488 | 1::100 | ThermoF | S-11223 | 2hrs RT |

| Type | Host | Fluorochrome | Dilution | Source | Catalog # | Incubation |
|---|---|---|---|---|---|---|
| 1° | Rat | - | 1::50 | BioRad | MCA497G | 15hrs at 4°C |
| 2° | Goat | AlexaFluor555 | 1::200 | ThermoF | A21434 | 2hrs RT |

**Table 8. Additional Staining.** Topro-3 Nuclear dye is used to identify the nucleus of cell in fluorescent microscopy. Fluorescent TRAP staining is used for the identification of osteoclasts, it is diluted in Trap Incubation Solution (TIS).

| | **Nuclear dye** | **Fluorescent TRAP** |
|---|---|---|
| **Fluorochrome** | **AF647** | **Excitation 405**<br>**Emission: 500** |
| **Dilution** | **1:10,000** | **4:1 in TIS** |
| **Incubation conditions** | **10 min RT** | **15 min RT under UV** |

## Confocal Microscopy

Immunofluorescent staining results are examined and scanned in a Zeiss 780 inverted microscope. The sections are acquired by tile scanning with 8-10 Z-stacks of 2μm thickness. Images are in Zen Blue Software and converted and quantified using the Imaris software for manual counting.

## Flow Cytometry

Flow cytometry can be used to identify and quantify individual cells based of cell surface markers. Fluorescence Activated Cell Sorting (FACS) uses lasers and antibodies conjugated with fluorescent markers to analyze and quantify cells of various tissues. Our tissue of interest typically includes blood, brain, liver, lung, kidney and bone marrow. Preparation for FACS experiment require single cell suspensions, in the section below we described this in further detail ("*Individual tissue preparation*").

### *Individual tissue preparation for FACS analysis*

**Bone marrow** → FACS buffer is created by adding 2.5g of bovine serum albumin (BSA) and 2 ml of EDTA in 500 ml of PBS buffer. The solution is filtered and kept on ice or stored at 4°C before using. Bone samples collected are cut with a scalpel at the epiphysis on both ends of the bone. A 10 ml syringe is filled with 10 ml of FACS buffer and is inserted in the shaft of the bone. The bone is held over a 10 ml tube as the FACS buffer is pushed through the shaft of the bone allowing the bone marrow to be collected in the tube. The bone marrow/FACS buffer is centrifuged at 320g and 4°C for 5 minutes. The

supernatant is disposed, and the pellet is resuspended with Ammonium-Chloride-Potassium (ACK) lysing buffer for 30 seconds. FACS buffer is added, and the mixture is centrifuged again to form a pellet. Following the disposal of the remaining supernatant, the cells are resuspended in FACS buffer in preparation for staining and analysis

**Blood** → Blood for FACS analysis is collected through the cardiac puncture method previously discussed. ACK lysis buffer is added to each tube of collected blood and left to incubate for 30 seconds before FACS buffer is added. The test tube mixture is then centrifuged at 320 g and 4°C for 5 minutes. After confirmation of pellet formation, supernatant is collected and moved to a clean tube. ACK lysis buffer is added to the tube once more and the proceeding steps are repeated. The resulting supernatant is disposed of, and the remaining pellet is resuspended in FACS buffer for staining and analysis.

**Soft tissues** → Soft tissues such as the brain, liver, lung and kidney collected through the previously described sample collection methods. A 24 well plate is prepared with 1 mL of PBS and 1mL of enzyme mix containing 3% FBS, 1mg/mL of Collagenase D, 0.2mg/mL of Dnase, and 2.4 mg/mL of Dispase II (**See Table 9**). Immediately after dissections, the soft tissue is kept in the PBS on ice until all the samples are collected. The tissues are then placed in the enzyme mix and cut into small pieces. They are left to incubate for 30 minutes at 37°C. Once sufficiently digested, the tissue mixture is put through a 100 μm cell strainer in 4ml of FACS buffer until the mixture is uniform. The mixture is centrifuged at 320 g and 4°C for 5 minutes, and the pellet is resuspended and

washed in FACS buffer. After a final spin down of the mixture. The pellet is resuspended in the decided final volume of FACS buffer.

**Table 9. Enzyme mix for digestion of soft tissue.** This mix is used for the breakdown of liver, lung, brain and kidney tissue. Organs are incubated in mix at 37°C for 30 minutes.

| Reagent | Catalog # | Company | Solvent | Final [C] |
|---|---|---|---|---|
| FBS | 10438026 | Thermofisher | - | 3% |
| Collagenase D | 11088882001 | Sigma Millipore | PBS | 1mg/ml |
| Dnase | DN25-100MG | Sigma Millipore | Dnase free H2O | 0.2mg/ml |
| Dispase II | 17105041 | Thermofisher | PBS | 2.4mg/ml |

*FACS analysis*

Single cell suspensions are stained with a series of antibodies for at least 30 minutes at 4°C before they are transferred to a 96 well plate (**See Table 10**). The final solution is filtered through a 100μm cell filter into a FACs tube. The samples are analyzed and quantified by the BD LSR Fortessa.

**Table 10. FACS Antibody list.** Antibodies used for FACS analysis of the different tissues from *CathepsinK$^{CreERT2;\ R26}$$^{LSL\text{-}YFP}$* **analyzed.**

***Tissue resident macrophages***

| ***CathepsinK$^{CreERT2;\ R26}$$^{LSL\text{-}YFP}$*** | | | | | |
|---|---|---|---|---|---|
| **Tissue** | **Antibody** | **Fluorochrome** | **Clone** | **Company/#** | **Final dilution** |
| Liver<br>Lung<br>Brain<br>Kidney | CD3 | APC-Cy7 | 145-2-C11 | Biolegend/100330 | 1:50 |
| | CD19 | APC-Cy7 | 6D5 | Biolegend/115530 | 1:50 |
| | Ter119 | APC-Cy7 | Ter-119 | Biolegend/116223 | 1:50 |
| | NkP46 | APC-Cy7 | 29A1.4 | Biolegend/137646 | 1:100 |
| | Ly6G | APC-Cy7 | 1A8 | Biolegend/127624 | 1:200 |
| | F4/80 | BV421 | BM8 | Biolegend/123132 | 1:50 |
| | CD11b | APC | M1/70 | Biolegend/101212 | 1:400 |
| | CD45 | PE | 30-F11 | Biolegend/103106 | 1:200 |
| | Ly6C | PECy7 | HK1.4 | Biolegend/128018 | 1:2000 |

***Blood Monocytes***

| **Tissue** | **Antibody** | **Fluorochrome** | **Clone** | **Company/#** | **Final [C]** |
|---|---|---|---|---|---|
| Blood | CD3 | APC-Cy7 | 145-2-C11 | Biolegend/100330 | 1:50 |
| | CD19 | APC-Cy7 | 6D5 | Biolegend/115530 | 1:50 |
| | Ter119 | APC-Cy7 | Ter-119 | Biolegend/116223 | 1:50 |
| | NkP46 | APC-Cy7 | 29A1.4 | Biolegend/137646 | 1:100 |
| | Ly6G | APC-Cy7 | 1A8 | Biolegend/127624 | 1:200 |
| | CD115 | APC | AFS98 | Biolegend/135510 | 1:100 |
| | CD11b | BV711 | M1/70 | Biolegend/101212 | 1:200 |
| | CD45 | PE | 30-F11 | Biolegend/103106 | 1:400 |
| | Ly6C | PECy7 | HK1.4 | Biolegend/128018 | 1:1000 |

***Bone Marrow***
Monocytes and Osteoprogenitor cells

| Tissue | Antibody | Fluorochrome | Clone | Company/# | Final [C] |
|---|---|---|---|---|---|
| BM | CD3 | APC-Cy7 | 145-2-C11 | Biolegend/10033 | 1:50 |
| | CD19 | APC-Cy7 | 6D5 | Biolegend/11553 | 1:50 |
| | Ter119 | APC-Cy7 | Ter-119 | Biolegend/11622 | 1:50 |
| | NkP46 | APC-Cy7 | 29A1.4 | Biolegend/13764 | 1:100 |
| | Ly6G | APC-Cy7 | 1A8 | Biolegend/12762 | 1:200 |
| | CD11b | BV711 | M1/70 | Biolegend/10121 | 1:200 |
| | CD117 | PE | 2B8 | Biolegend/10580 | 1:800 |
| | CD45 | Pacific Blue | 30-F11 | Biolegend/10310 | 1:400 |
| | CD115 | APC | AFS98 | Biolegend/13551 | 1:100 |
| | Ly6C | PECy7 | HK1.4 | Biolegend/12801 | 1:400 |

***Bone Marrow***
Hematopoietic progenitors (HSCs)

| Tissue | Antibody | Fluorochrome | Clone | Company/# | Final [C] |
|---|---|---|---|---|---|
| BM | CD3 | APC-Cy7 | 145-2-C11 | Biolegend/100330 | 1:50 |
| | CD19 | APC-Cy7 | 6D5 | Biolegend/115530 | 1:50 |
| | NkP46 | APC-Cy7 | 29A1.4 | Biolegend/137646 | 1:100 |
| | Ter119 | APC-Cy7 | Ter-119 | Biolegend/116223 | 1:100 |
| | Gr-1 | APC-Cy7 | RB6-8C5 | Biolegend/108424 | 1:200 |
| | CD11b | APC-Cy7 | M1/70 | Biolegend/101226 | 1:200 |
| | Sca-1 | Pacific Blue | D7 | Biolegend/108120 | 1:50 |
| | CD45 | PECy7 | 30-F11 | Biolegend/103114 | 1:800 |
| | CD117 | PE | 2B8 | Biolegend/105808 | 1:800 |

## Paraffin Histology

*Tissue processing*

Following the previously described sample collection methods, the samples are fixed in 4% formaldehyde solution for 3 days. Bone samples are then decalcified in 14% EDTA for 10 days with changes of the solution every 10 days. The samples are stored in 70% EtOH until tissue processing.

**Table 11. Tissue processing guide for samples.**

| Position | Solution | Time |
|---|---|---|
| 1 | 70% EtOH | 1 hour |
| 2 | 85% EtOH | 1 hour |
| 3 | 95% EtOH | 1 hour |
| 4 | 95% EtOH | 1 hour |
| 5 | 100% EtOH | 1.5 hours |
| 6 | 100% EtOH | 1.5 hours |
| 7 | 100% EtOH | 1.5 hours |
| 8 | Xylene | 1.5 hours |
| 9 | Xylene | 1.5 hours |
| 10 | Xylene | 1.5 hours |
| 11 | Paraffin bath | 2 hours |
| 12 | Paraffin bath | 2 hours |

Tissue processing for paraffin histology is a process used to modify the density and texture of a tissue so that it is more aligned with the properties of the paraffin wax. This allows for easier cutting of sections for staining. The process starts by leaving the sample in 70% Ethanol for at least 24hrs. Following this, the samples are placed in the Sakura Tissue Tek VIP E150 tissue processor. In an attempt to push out as much liquid as possible from the tissues, the samples will be run through solutions of increasing concentration of Ethanol before being moved to Xylene (**See Table 11**). The samples are then kept in a paraffin bath with infiltrating wax for the tissues to absorb wax before being embedded.

## Trap Staining

Tartrate-Resistant Acid Phosphatase (TRAP) staining is a method used to for staining of osteoclast. The process begins with warming slides containing the paraffin sections at 50°C for one hour. In preparation for TRAP staining, the samples are deparaffinized through a series of incubations in several solutions (**See Table 12**). The mixture is then incubated at 37°C in a Basic Stock Incubation Solution/Naphthol-Ether Substrate solution for one hour. Following this step, the slides are moved to a Basic Stock Solution/Sodium Nitrite/Basic Fuchsin solution for 2 minutes at 37°C for TRAP Staining. After a few washes with water, the slides are counterstain with a 1:10 hematoxylin solution for 2 minutes. The slides are put through a dehydration and subsequently mounted with Entellan (**See Table 12**).

**Table 12. Deparaffinization Sequence and Dehydration Sequence.** Samples are deparaffinized to make the tissue embedded more receptive to the staining performed. Samples are subsequently dehydrated before mounting.

| **Deparaffinization Sequence** | | **Dehydration Sequence** | |
|---|---|---|---|
| Xylene | 5 minutes | 50% Ethanol | 1 minute |
| Xylene | 5 minutes | 70% Ethanol | 1 minute |
| 100% Ethanol | 3 minutes | 95% Ethanol | 1 minute |
| 100% Ethanol | 3 minutes | 95% Ethanol | 1 minute |
| 95% Ethanol | 3 minutes | 100% Ethanol | 1 minute |
| 70% Ethanol | 3 minutes | 100% Ethanol | 1 minute |
| 50% Ethanol | 3 minutes | Xylene | 1 minute |

## Osteoclast Quantification

TRAP-stained osteoclasts are identified and quantified through a Leica microscope. Pictures are taken of several sections of the bone, focusing on the trabecular area. Images are then stitched together on Photoshop for a complete image of the bone. Using ImageJ, the trabecular area is calculated, and the identified multinucleated osteoclast are counted individually.

# RESULTS

## *Tamoxifen inducible Cx3cr1$^{CreERT2}$; Braf$^{LSL\text{-}V600E}$ mouse model*

Prior research investigated the labeling efficiency of EMP cells in the reporter mouse *Cx3cr1$^{CreERT2}$;Rosa26$^{LSL\text{-}YFP}$* [24]. These mice were examined through frozen histology and FACS analysis. This determined that the expression of the YFP fluorescent protein was restricted to tissue resident macrophages and EMP derived (embryonic) osteoclasts. Once the inducible Cre recombination and fluorescent labeling of the *Cx3cr1$^{CreERT2}$* mouse was confirmed to be specific, the next step was to induce the *Braf$^{V600E}$* mutation to generate a potential mouse model for histiocytic- like disease with multisystemic presentation and bone involvement. Since the Cx3cr1 marker labels all EMP derived cells, when induced with 4OHT at E10.5, it was expected that this induction would produce the desired phenotype in mice.

A cross between a *Cx3cr1$^{CreERT2}$* mouse and a *Braf$^{LSL\text{-}V600E}$* mouse was performed, and pregnant dams were injected with 37.5ug/g of tamoxifen supplemented with 18.75ug/g of progesterone mixture at E10.5. The resulting embryos were harvested at E18.5.

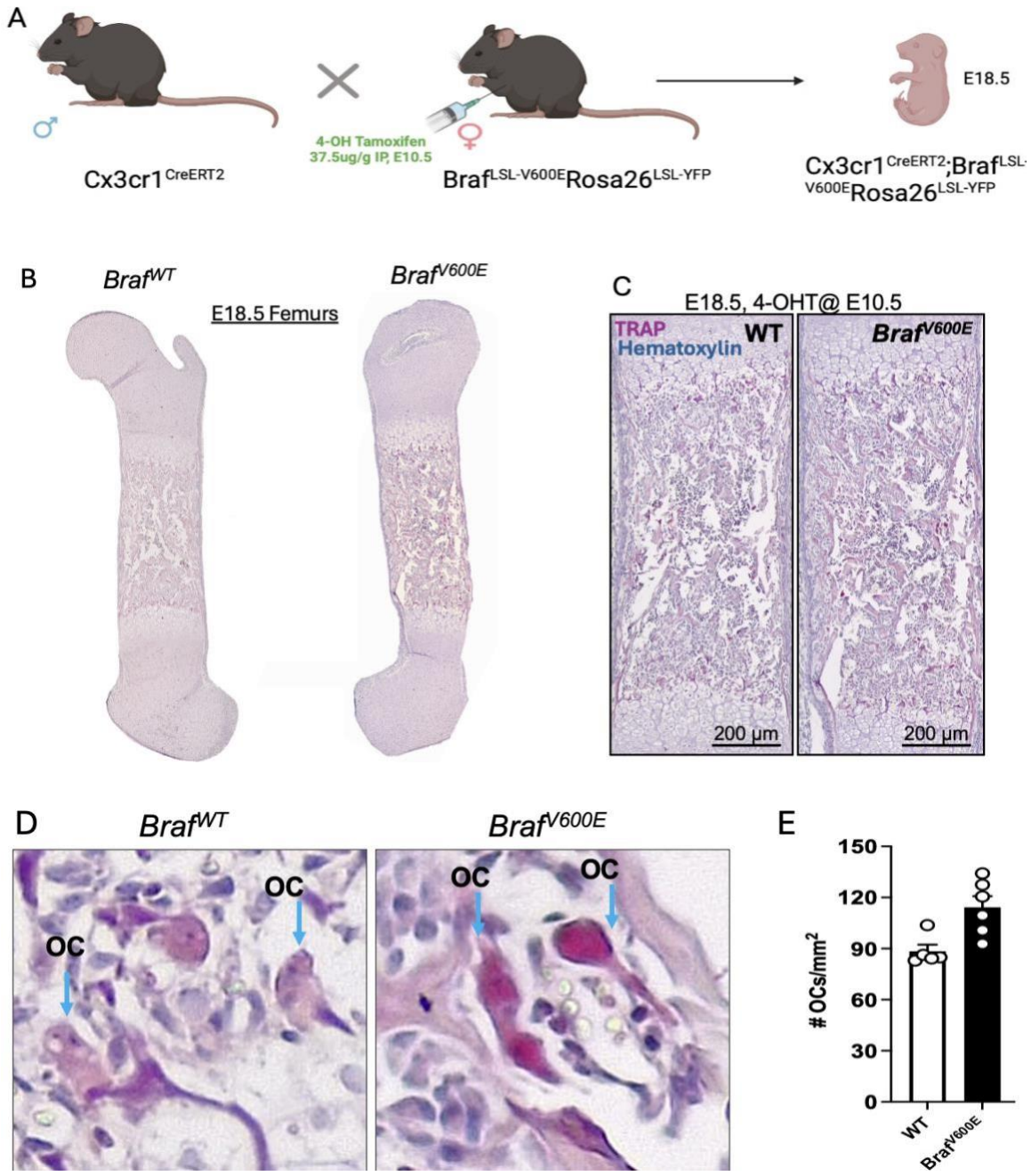


**Figure 3. Analysis of *Cx3cr1$^{CreERT2}$; Braf$^{LSL-V600E}$* E18.5 embryos.** (3A) Breeding schema for generation of the embryo analyses. (3B) Embryonic femur paraffin sections stained with TRAP and hematoxylin. (3C) Trabecular bone view. (3D) WT and Braf+ OCs marked. (3E) Quantification of OCs WT and Braf+ per trabecular area. Data represents 5 (WT)or 6 (BRAF) biological replicates with 3 sections each mouse. Statistical analysis was unpaired T-test with a P value of 0.0105.

The embryonic samples collected were processed for paraffin histology for analysis of femur sections. The number of osteoclasts were counted for each section with the $Cre^-$ litter mates serving as controls. Through our analysis, we found that the $Cre^+$ BrafV600E+ mice displayed a greater number of osteoclasts in ossification centers at E18.5 compared to Braf– mice negative littermate control embryos. The hallmark of histiocytosis is aberrantly active osteoclasts. The difference in the osteoclasts number quantified between genotypes signifies the possibility of correlation with osteoclast number and the bone resorption activity observed in histiocytic bone lesions. However, since bone mineralization occurs postnatally and gradually during development, we couldn't determine whether this will result in bone loss and/or bone lesions. These experiments are under continued investigation.

### *Unpulsed $Ctsk^{Cre};R26^{LSL\text{-}YFP}$*

*$Ctsk^{Cre};$* $R26^{LSL\text{-}YFP}$ mice samples were collected at either P12 as pups or 3-6 weeks as adult mice. The lungs. brain, liver and kidney were collected for analysis of labeling in tissue resident macrophages. Additionally, peripheral blood and bone marrow were collected for the analysis of HSCs derived cells. FACS analysis was performed to determine the viability of the model. The use of the Cre/LoxP system requires confirmation of non-labeling in the constitutive system. The goal is to rule out spontaneous Cre recombination without pulsing of tamoxifen.

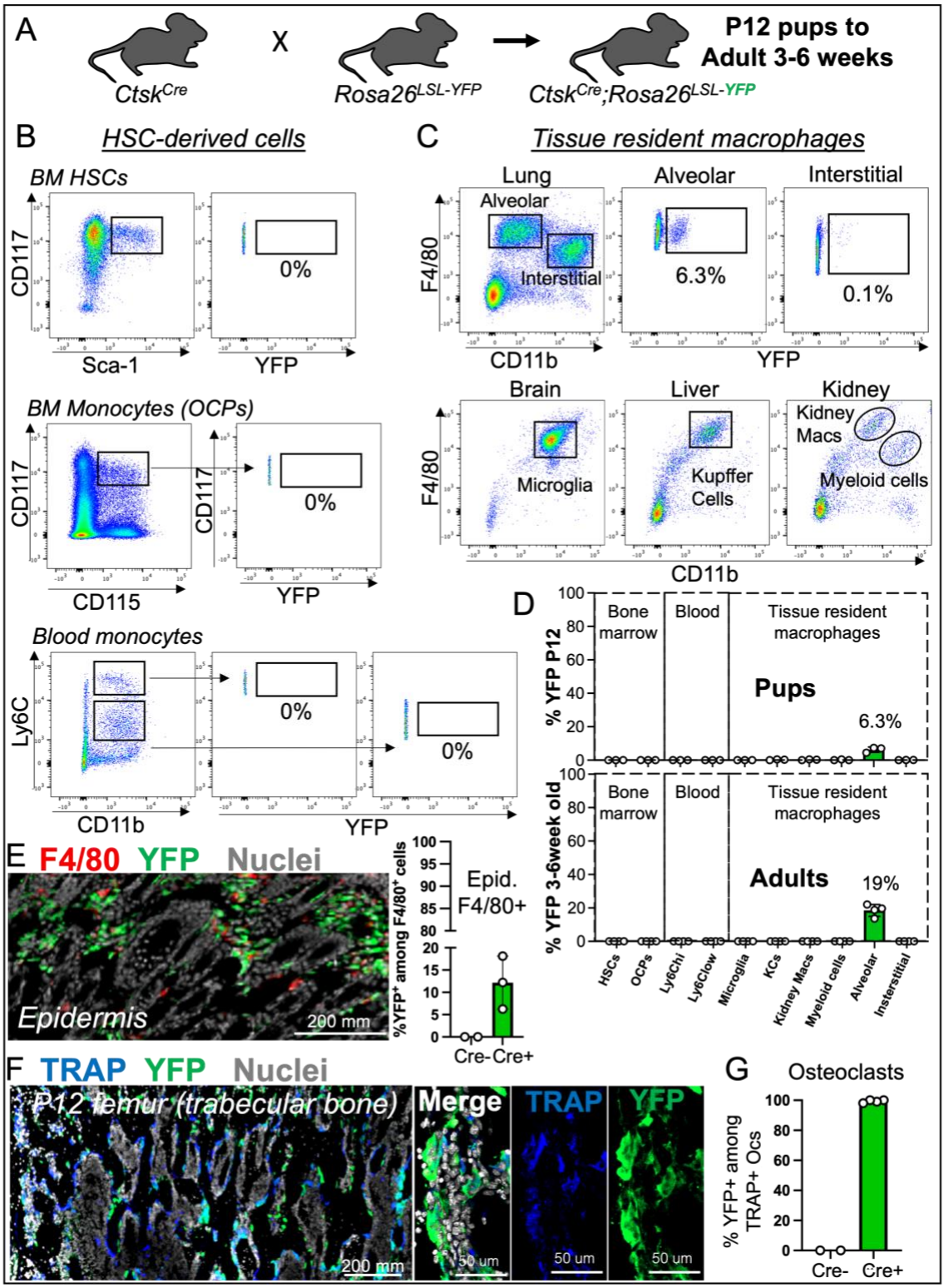
A
Ctsk^Cre
X
Rosa26^LSL-YFP
Ctsk^Cre;Rosa26^LSL-YFP
P12 pups to Adult 3-6 weeks
B
HSC-derived cells
BM HSCs
CD117
Sca-1
0%
YFP
BM Monocytes (OCPs)
CD115
Blood monocytes
Ly6C
CD11b
C
Tissue resident macrophages
Lung
Alveolar
Interstitial
F4/80
CD11b
6.3%
0.1%
YFP
Brain
Liver
Kidney
Microglia
Kupffer Cells
Kidney Macs
Myeloid cells
D
% YFP P12
Bone marrow
Blood
Tissue resident macrophages
Pups
6.3%
% YFP 3-6week old
Adults
19%
HSCs
OCPs
Ly6Chi
Ly6Clow
Microglia
KCs
Kidney Macs
Myeloid cells
Alveolar
Insterstitial
E
F4/80 YFP Nuclei
Epidermis
200 mm
%YFP+ among F4/80+ cells
Epid. F4/80+
Cre-
Cre+
F
TRAP YFP Nuclei
P12 femur (trabecular bone)
200 mm
Merge
TRAP
YFP
50 um
G
Osteoclasts
% YFP+ among TRAP+ Ocs
Cre-
Cre+

**Figure 4. Analysis of *Cathepsin-k$^{Cre}$; Rosa26$^{LSL-YFP}$*.** (4A) Breeding Schema for mice. (4B) FACS analysis of HSC derived cells. (4C) FACS analysis of tissue resident macrophages. (4D) Percentage of YFP+ cells in P12 pups and adult mice. (4E) F4/80, YFP, To-pro- 3 staining of skin section). (4F) P12 trabecular bone section stained with TRAP, YFP and To-pro-3. (4G) Percentage of YFP+ osteoclasts in Cre- and Cre+ mice. N=3 for P12 pups, N=4 for 3–6-week-old mice.

FACS analysis of bone marrow looked at YFP expression in HSCs and monocytes/osteoclast progenitor cells. Peripheral blood collected was also examined for the expression of YFP in monocytes or Ly6C$^+$ cells. There was no YFP labeling found within these cells. Following this, tissues collected were examined for percentage of labeling of tissue resident macrophages. Approximately 6% of alveolar macrophages, which are EMP-derived macrophages of the lung, were labeled. Examining other tissues, no YFP labeling was found in either microglia, Kupffer cells, kidney macrophages or myeloid cells. Comparing differences of the labeling efficiency percentage of YFP between the P12 pups and the 3-6 weeks adult mice, there was a 3-fold increase in the percentage of YFP labeling efficiency in older mice, suggesting that this population of embryonic macrophages increase proportionally with aging. We have not yet analyzed older mice to determine increase.

Additionally, femur sections stained with fluorescent TRAP, anti GFP and To-Pro- 3 nuclear stain were examined for the percentage of YFP labeling. In P12 Cre+ femur, the number of osteoclasts in the trabecular bone was quantified for efficiency in labeling osteoclast. It was determined that 99-100% of osteoclast in Cre+ mice were labeled with the YFP fluorescent protein. This was compared to the Cre-

control which did not show any YFP+ signal. This confirms *Ctsk*$^{Cre;}$ R26$^{LSL\text{-}YFP}$ as a viable non-leaky model for the labeling of osteoclast with an inducible Cre/LoxP system. Epidermis F4/80+ macrophages also showed up to 20% of YFP labeling, however, we also noticed there were F4/80 negative cells that were YFP+, suggesting other cells beyond macrophages express YFP.

### *Pulsed Ctsk*$^{CreERT2;}$*R26*$^{LSL\text{-}YFP}$

With the confirmation that spontaneous Cre recombination does not occur in the *Ctsk*$^{Cre;}$*R26*$^{LSL\text{-}YFP}$ model, we looked to examine the effectives of an inducible Cre model. A *Ctsk*$^{CreERT2}$ mouse is crossed with a R26$^{LSL\text{-}YFP}$ mouse to produce a *Ctsk*$^{CrERT2;}$ R26$^{LSL\text{-}YFP}$ pup. These pups are injected at P7 or P8 with a 200 ug/g 4OH-Tamoxifen and 100 ug/g progesterone mixture. P7 pups were injected first and samples were collected from them 4 days later. Immunofluorescent analysis showed a disproportionate labeling of mononuclear cells and very few osteoclasts. Due to the abundance of mononuclear cells, we hypothesized that the mononuclear cells had not been given enough time to fuse and create mature osteoclasts. The average percentage of YFP+ osteoclast was approximately 24.4%.

Following these results, we sought to increase the labeling efficiency of the model. We injected P8 mice and proceeded to collect samples from them 7 days later instead of 4. We found that percent of YFP+ osteoclasts had increased to an average of 27.2%. This provided us with an idea of the labeling efficiency of one pulse of tamoxifen. Due to the relatively low frequency of fusion events for the formations of

osteoclasts, we decided that multiple pulses of tamoxifen could provide a model that would potentially display a higher percentage of labeling.

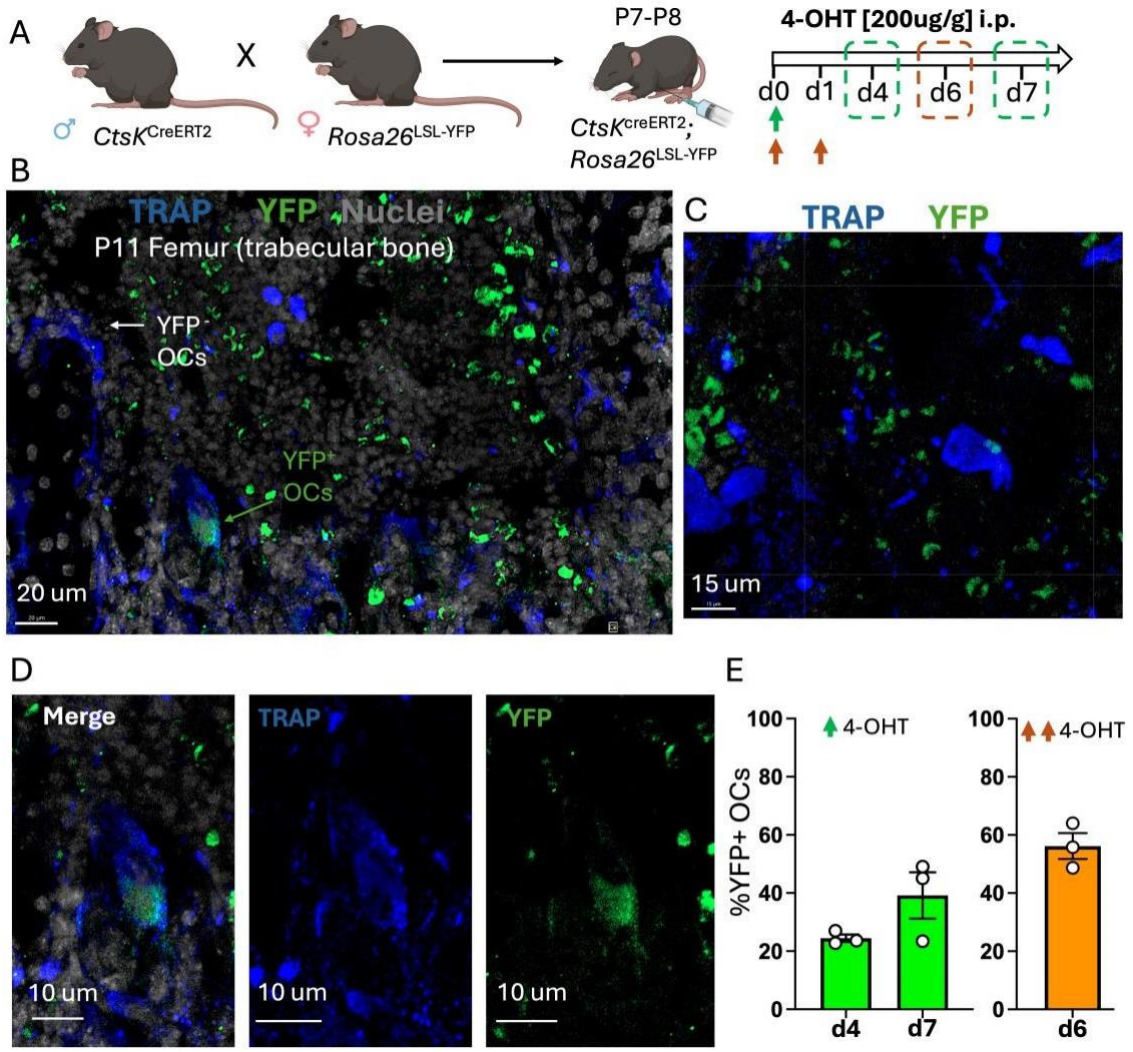


**Figure 5. Analysis of pulsed *Ctsk$^{CreERT2}$; R26$^{LSL-YFP}$* mice.** (5A) Breeding schema for generation of experimental mice. (5B) P15 trabecular bone section of a femur. (5C) Fusion event of YFP+ cell with YFP- osteoclast. (5D) YFP+ osteoclast. (5E) Percentage of YFP+ labeling in osteoclasts in P7-P8 pups (d0) injected with 4-OHT at the respective time points of analysis (N=3 for all time points, and 2-3 femur sections

Some literature reports success with multiple pulses of tamoxifen during a period of 7 days. As tamoxifen can be extremely toxic, we attempted to titrate of suitable amount to achieve the percentage of labeling desired while avoiding potential expiration of the mice due to sickness. The next litter of mice was injected at P7 with the standard protocol dose of the 200 ug/g 4OH-Tamoxifen and 100 ug/g progesterone mixture. The mice were weighed before each injection and monitored carefully for signs of sickness. The mice did not showcase any complication after the first dose of tamoxifen and were relatively on par with their non-injected litter mates in terms of development. The second dose of the 200 ug/g 4OH-Tamoxifen and 100 ug/g progesterone mixture was administered 24hrs later (d1) with the goal of collecting samples from the mice after one week. Around P11-P12, the mice began to display signs of sickness and they did not gain any more weight in comparison to wild-type littermate controls samples were taken at P12 (d6).

# DISCUSSION

## *Cx3cr1$^{CreERT2}$; Braf$^{LSL\text{-}V600E}$*

Post-natal mice that carry the *Braf$^{V600E}$* mutation often display visible phenotypic differences with wildtype mice. Due to the samples being collected as embryo, these differences could not be fully characterized, however, this is currently under investigation to determine adult phenotypes. The pulsed *Cx3cr1$^{CreERT2}$; Braf$^{LSL\text{-}V600E}$* provided us with an inducible model in which osteoclasts frequency in the trabecular bone area increased in Braf+ mice. While this is a significant finding, secondary analysis such as osteoclast nuclei quantification and examination of post-natal mice would be beneficial for confirmation of the validity of this model.

The labeling in the pulsed *Cx3cr1$^{CreERT2}$; Braf$^{LSL\text{-}V600E}$* model was highly specific to the EMP derived cells. This allows for the marking of tissue resident macrophages and EMP derived osteoclasts. Since organ specific lesions tend to be formed by the tissue resident macrophages of that organ, this model could be useful for the study of multisystem histiocytosis. However, osteoclasts can be derived from both EMPs and HSCs. If this model is used for the study of histiocytic bone lesions, only the EMP derived osteoclast express the mutation, therefore, is expected that bone phenotype observed in E18.5 embryos will only be detected in early bone development and just within few weeks after birth (yet to be determined) since HSC-derived monocytes replace embryonic osteoclasts gradually.

### *Ctsk$^{CreERT2}$;R26$^{LSL\text{-}YFP}$*

This model was able to produce adequately efficient inducible labeling of osteoclasts with just a single dose (and expected higher efficiency with further doses). Based on the results we can infer that collecting samples one week from the first injection is an ideal time frame for labeled Cathepsin-K+ mononuclear precursors that will fuse with osteoclasts. Although the labeling efficiency from one pulse of 4OH-tamoxifen is promising, there is the possibility that multiple pulses of 4OH-tamoxifen could further raise the labeling efficiency of osteoclasts in these pups. The concern is that the pups do not respond well to multiple injections of tamoxifen due to toxicity of this chemical with the tested protocols. However, we are currently working on optimization of the dose response for maximal Cre recombination efficiency while keeping toxicity to a minimum.

Notably the pups injected once and examined for one week did not show any signs of sickness. This brings forth the idea of potentially mitigating the toxicity of tamoxifen by increasing the time between each injection and possibly reducing consecutive doses, this would also allow enough time for the pups to absorb and metabolize each tamoxifen injection and recover from potential toxicity of tamoxifen. These experiments will potentially provide an experimental plan to generate a new model for multisystem histiocytosis with a bone phenotype, *Cathepsin-K$^{CreERT2}$;Braf$^{LSL\text{-}V600E}$*, that can be useful to study pathological mechanisms of histiocytosis and for drug testing.

## LIST OF JOURNAL ABBREVIATIONS

*Ann Diagn Pathol*.....Annals of Diagnostic Pathology

*Ann Med Surg*.....Annals of Medicine and Surgery

*Dev Camb Engl*.....Development Cambridge England

*Endocr Connect*.....Endocrine Connections

*Future Sci OA*.....Future Science: Open Access

*Insights Imaging*.....Insights into Imaging

*Int J Mol Sci*.....International Journal of Molecular Sciences

*J Clin Endocrinol Metab*.....Journal of Clinical Endocrinology & Metabolism

*J Clin Oncol*.....Journal of Clinical Oncology

*J Exp Med*.....Journal of Experimental Medicine

*Med. J Hem.Infec.Dis*.....Mediterranean Journal of Hematology and Infectious Diseases

*Methods Mol Biol*.....Methods in Molecular Biology

*Mod Pathol Off J U S Can Acad Pathol Inc*.....Modern Pathology

*N Engl J Med*.....New England Journal of Medicine

*Nat Med*.....Nature Medicine

*Pediatr Blood Cancer*.....Pediatric Blood Cancer

*PloS One*.....Public Library of Science One

*Sci Rep*.....Scientific Reports

*Trends Immunol*.....Trends in Immunology

## BIBLIOGRAPHY


1. Allen CE, Merad M, McClain KL. Langerhans-Cell Histiocytosis. *N Engl J Med*. 2018;379(9):856-868. doi:10.1056/NEJMra1607548

2. Haupt R, Minkov M, Astigarraga I, et al. Langerhans cell histiocytosis (LCH): guidelines for diagnosis, clinical work-up, and treatment for patients till the age of 18 years. *Pediatr Blood Cancer*. 2013;60(2):175-184. doi:10.1002/pbc.24367

3. Khung S, Budzik JF, Amzallag-Bellenger E, et al. Skeletal involvement in Langerhans cell histiocytosis. *Insights Imaging*. 2013;4(5):569-579. doi:10.1007/s13244-013-0271-7

4. Javadi T, Hill C, McLemore ML, Oskouei S, Bahrami A. Adult-onset Langerhans cell histiocytosis of bone: A case series highlighting a rare entity. *Ann Diagn Pathol*. 2023;66:152171. doi:10.1016/j.anndiagpath.2023.152171

5. Kamal AF, Luthfi APWY. Diagnosis and treatment of Langerhans Cell Histiocytosis with bone lesion in pediatric patient: A case report. *Ann Med Surg*. 2019;45:102-109. doi:10.1016/j.amsu.2019.07.030

6. Anastasilakis AD, Tsoli M, Kaltsas G, Makras P. Bone metabolism in Langerhans cell histiocytosis. *Endocr Connect*. 2018;7(7):R246-R253. doi:10.1530/EC-18-0186

7. Wick MR, McDermott MB, Swanson PE. Proliferative, reparative, and reactive benign bone lesions that may be confused diagnostically with true osseous neoplasms. Published online January 2014. doi:10.1053/j.semdp.2013.12.002

8. Chellapandian D, Makras P, Kaltsas G, et al. BISPHOSPHONATES IN LANGERHANS CELL HISTIOCYTOSIS: AN INTERNATIONAL RETROSPECTIVE
CASE SERIES. *Mediterr J Hematol Infect Dis*. 2016;8:2016033. doi:10.4084/mjhid.2016.033

9. Cantu MA, Lupo PJ, Bilgi M, Hicks MJ, Allen CE, McClain KL. Optimal therapy for adults with Langerhans cell histiocytosis bone lesions. *PloS One*. 2012;7(8):e43257. doi:10.1371/journal.pone.0043257

10. Watts NB, Diab DL. Long-Term Use of Bisphosphonates in Osteoporosis. *J Clin Endocrinol Metab*. 2010;95(4):1555-1565. doi:10.1210/jc.2009-1947

11. Kasaai B, Caolo V, Peacock HM, et al. Erythro-myeloid progenitors can differentiate from endothelial cells and modulate embryonic vascular remodeling. *Sci Rep*. 2017;7(1):43817. doi:10.1038/srep43817

12. Mass E, Jacome-Galarza CE, Blank T, et al. A somatic mutation in erythro-myeloid progenitors causes neurodegenerative disease. *Nature*. 2017;549(7672):389-393. doi:10.1038/nature23672

13. Yahara Y, Nguyen T, Ishikawa K, Kamei K, Alman BA. The origins and roles of osteoclasts in bone development, homeostasis and repair. *Dev Camb Engl*. 2022;149(8):dev199908. doi:10.1242/dev.199908

14. Jacome-Galarza CE, Percin GI, Muller JT, et al. Developmental origin, functional maintenance and genetic rescue of osteoclasts. *Nature*. 2019;568(7753):541-545. doi:10.1038/s41586-019-1105-7

15. Davies H, Bignell GR, Cox C, et al. Mutations of the BRAF gene in human cancer. *Nature*. 2002;417(6892):949-954. doi:10.1038/nature00766

16. Ottaviano M, Giunta EF, Tortora M, et al. BRAF Gene and Melanoma: Back to the Future. *Int J Mol Sci*. 2021;22(7):3474. doi:10.3390/ijms22073474

17. Héritier S, Emile JF, Barkaoui MA, et al. BRAF Mutation Correlates With High-Risk Langerhans Cell Histiocytosis and Increased Resistance to First-Line Therapy. *J Clin Oncol*. 2016;34(25):3023-3030. doi:10.1200/JCO.2015.65.9508

18. Cheng L, Lopez-Beltran A, Massari F, MacLennan GT, Montironi R. Molecular testing for BRAF mutations to inform melanoma treatment decisions: a move toward precision medicine. *Mod Pathol Off J U S Can Acad Pathol Inc*. 2018;31(1):24-38. doi:10.1038/modpathol.2017.104

19. Barré-Sinoussi F, Montagutelli X. Animal models are essential to biological research: issues and perspectives. *Future Sci OA*. 2015;1(4):FSO63. doi:10.4155/fso.15.63

20. Berres ML, Lim KPH, Peters T, et al. BRAF-V600E expression in precursor versus differentiated dendritic cells defines clinically distinct LCH risk groups. *J Exp Med*. 2014;211(4):669-683. doi:10.1084/jem.20130977

21. Bigenwald C, Le Berichel J, Wilk CM, et al. BRAFV600E-induced senescence drives Langerhans cell histiocytosis pathophysiology. *Nat Med*. 2021;27(5):851- 861. doi:10.1038/s41591-021-01304-x

22. Shi J, Hua L, Harmer D, Li P, Ren G. Cre Driver Mice Targeting Macrophages. *Methods Mol Biol Clifton NJ*. 2018;1784:263-275. doi:10.1007/978-1-4939-7837-3_24

23. Zhong ZA, Sun W, Chen H, et al. Optimizing tamoxifen-inducible Cre/loxp system to reduce tamoxifen effect on bone turnover in long bones of young mice. *Bone*. 2015;81:614-619. doi:10.1016/j.bone.2015.07.034

24. Hacein-Bey C. A MURINE MODEL FOR LABELING OF EMP-DERIVED MACROPHAGES AND OSTEOCLASTS.

25. Lee SE, Rudd BD, Smith NL. Fate-mapping mice: new tools and technology for immune discovery. *Trends Immunol*. 2022;43(3):195-209. doi:10.1016/j.it.2022.01.004

26. Taylor JA. EXPRESSION OF BRAF V600E MUTATION IN OSTEOCLASTS: A MURINE MODEL OF BONE EROSION IN HISTIOCYTOSIS-LIKE DISEASE.

# CURRICULUM VITAE